LEVEL II

EXPERIMENTAL STUDY OF THE EFFECTS OF FAULTS ON SPHERICAL WAVE PROPAGATION, PHASE I

J. C. Cizek, A. L. Florence,
D. D. Keough, and J. T. Rosenberg

SRI International
333 Ravenswood Avenue
Menlo Park, California 94025

October 1979

Final Report

Sponsored by

Defense Advanced Research Projects Agency (DoD)
DARPA Order No. 3749
Monitored by: LTC G. Bulin
under Contract No. DNA 001-79-C-0261

SRI International
333 Ravenswood Avenue
Menlo Park, California 94025
(415) 326-6200
Cable: SRI INTL MPK
TWX: 910-373-1246

UNCLASSIFIED

(9) Final rept. 29 Mar-30 Sep 79 on Phase 1,

SECURITY CLASSIFICATION OF THIS PAGE (When Data Entered)

REPORT DOCUMENTATION PAGE	READ INSTRUCTIONS BEFORE COMPLETING FORM
1. REPORT NUMBER / 2. GOVT ACCESSION NO.	3. RECIPIENT'S CATALOG NUMBER
(6) 4. TITLE (and Subtitle): EXPERIMENTAL STUDY OF THE EFFECTS OF FAULTS ON SPHERICAL WAVE PROPAGATION	5. TYPE OF REPORT & PERIOD COVERED: Final Report for Period 29 March - 30 Sept. 1979
	6. PERFORMING ORG. REPORT NUMBER: SRI PYU-8392
(10) 7. AUTHOR(s): J. C. Cizek, D. D. Keough, A. L. Florence, J. T. Rosenberg	(15) 8. CONTRACT OR GRANT NUMBER(s): DNA 001-79-C-0261, DARPA Order-3749
9. PERFORMING ORGANIZATION NAME AND ADDRESS: SRI International, 333 Ravenswood Avenue, Menlo Park, California 94025	10. PROGRAM ELEMENT, PROJECT, TASK AREA & WORK UNIT NUMBERS: DARPA Order No. 3749, Program Code No. 9D60, Program Element 61101E
11. CONTROLLING OFFICE NAME AND ADDRESS: Defense Nuclear Agency, Headquarters, Washington, D.C. 20305	(11) 12. REPORT DATE: Oct 1979
	13. NUMBER OF PAGES: 34 (12) 35
14. MONITORING AGENCY NAME & ADDRESS (if different from Controlling Office)	15. SECURITY CLASS (of this report): Unclassified
	15a. DECLASSIFICATION/DOWNGRADING SCHEDULE

16. DISTRIBUTION STATEMENT (of this Report)

Approved for public release; distribution unlimited.

17. DISTRIBUTION STATEMENT (of the abstract entered in Block 20, if different from Report)

18. SUPPLEMENTARY NOTES

19. KEY WORDS (Continue on reverse side if necessary and identify by block number)

Spherical waves
Faults
Plasticity
Explosives

20. ABSTRACT (Continue on reverse side if necessary and identify by block number)

A laboratory technique has been developed for investigating the effect on a spherical wave of a fault located close to a spherical explosive charge that is detonated to generate the wave. The medium is a grout that simulates tuff, the fault is idealized by Mylar sheets, and the sensor is a particle velocity gage. The gage principle is based on Faraday's law in that a voltage is induced in a conducting loop when a moving portion of the loop cuts the flux lines of a magnetic field.

→ over

DD FORM 1 JAN 73 1473 / EDITION OF 1 NOV 65 IS OBSOLETE

410281

UNCLASSIFIED

SECURITY CLASSIFICATION OF THIS PAGE (When Data Entered)

JCB

20. ABSTRACT

A measure of the wave-fault interaction was obtained by comparing records of particle velocity gages engulfed by waves that have not crossed faults with records of gages engulfed by waves that have crossed faults. From these comparisons, it was concluded that the technique is suitable for investigating wave-fault interactions.

CONTENTS

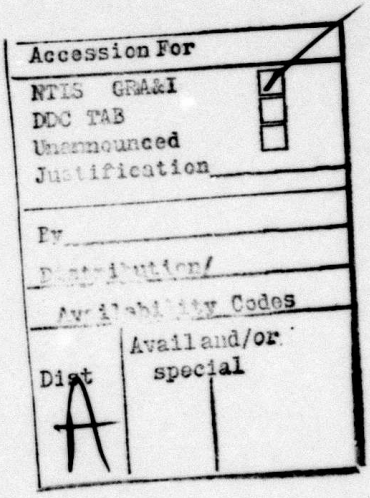

ACKNOWLEDGMENTS

The authors are indebted to the following personnel of SRI International for their assistance in the investigation: L. Seaman for calculations with the SRI PUFF computer code to estimate particle velocities, B. Lew for calculations to evaluate the mutual inductance particle velocity gage, A. Bartlett and L. Dary for fabricating the models, and L. Hall for performing the electronic aspects of the experiments.

1. INTRODUCTION

An important consideration in the detection of underground nuclear explosions is the effect on the spherical wave propagation of medium asymmetries, such as geological faults, located near the energy source. The assumption of spherical symmetry for calculations has the advantage that it frequently allows tractable formulation and solution of the wave problem, but the results may be too approximate or even misleading because of the asymmetry effect.

As a means of investigating asymmetry in this context, we designed a laboratory technique and applied it to the case of a simplified planar fault. This technique is described fully in Section 2, but briefly the apparatus consists of a small spherical explosive source cast in a cylinder of rock-matching grout. The fault consists of two parallel planar sheets of Mylar also cast in the grout and located next to the charge in the final plastic zone. The spherical wave that is generated on detonation of the charge is monitored by two particle velocity gages. The gages are located on either side of the charge so that one gage receives a part of the wave that has not crossed the fault, whereas the other gage receives a part of the wave that has crossed the fault.

Five experiments were performed, four of which were successful. Detailed results are presented in Section 3. In the first two experiments, no faults were included so that we could establish the standard spherical wave. Four similar particle velocity records were obtained. In the last three experiments, faults were included. In two of these three experiments particle velocity records were obtained. The gages that received a part of the wave that did not cross the fault provided records similar to the four records from the first two experiments. The gages that received a part of the wave that did cross the fault provided records of similar overall shape (velocity versus time) but with a 32%

lower peak particle velocity in one test and 9% in the other. In the third test with a fault, the principal characteristics of the particle velocities appear, but noise in the form of an instantaneous voltage shift in both records prevented determination of the particle velocities. A reasonable assumption about this noise behavior reproduced, upon subtraction, a particle velocity ratio similar to those obtained from the other fault tests.

We conclude from the above results that an experiment has been devised that is suitable for investigating the effect on spherical waves of asymmetries in the neighborhood of an energy source.

2. EXPERIMENTAL TECHNIQUE

2.1 General Description

Figures 1 and 2 show schematically two views of the experimental apparatus including the sensors for the initial symmetry experiments. A 3/8-gram charge of PETN explosive contained in a thin-walled spherical shell of Lucite (Figure 3) is cast in the center of a rock-matching grout cylinder, 11 inches (27.9 cm) in diameter and 11 inches (27.9 cm) high. The grout, designated RMG 2C4, matches the properties of Nevada Test Site tuff. We chose this material for our feasibility study because it is well characterized and because of our experience in using it for laboratory investigations of containment of underground nuclear explosions.[1] The 3/8-gram charge was also developed for the containment studies, and it has been shown to produce waves that are reproducible.

Figures 1 and 2 also show two embedded particle velocity gages. Part of this feasibility study consisted of choosing the type of particle velocity gage from two candidates: the external field gage (EF gage) and the mutual inductance gage (MI gage). This study resulted in the choice of the EF gage. The reasons for finding the MI gage unsuitable are given in the Appendix. The external field required for the EF gage was provided by a solenoid surrounding the grout cylinder, the wire being wound on a thin-walled PVC cylindrical shell of 11-3/8 inches (28.9 cm) internal diameter to provide 86 turns in a height of 11-1/2 inches (29.2 cm). A constant magnetic field of 1506 Gauss (0.1506 W/m^2) was measured by two embedded Hall probes included in each test. This field was generated by a direct current of 416 A flowing through the coil powered by 8 automobile batteries, each having a nominal voltage of 12 V, connected in series to provide a measured voltage of 101 V. Each Hall probe produced 60mV/k Gauss, a value obtained by calibration in a standard magnetic field. The Hall probes were located in the midheight plane of the grout

cylinder at the same radius as the active elements of the EF gages; this radius was 4 cm in each test.

An approximate verification of the field strength is provided by the theoretical prediction of the field within an infinitely long solenoid. If n is the number of turns per meter and I is the current in amperes, then the field B in Webers/m^2 is

$$B = 4\pi \cdot 10^{-7} \cdot nI$$

For m = 295 turns/m and I = 416 A, the field is

$$B = 0.154 \text{ W/m} = 1540 \text{ Gauss}$$

Figures 4 and 5 show schematically two views of the experimental apparatus for the asymmetry experiments. The configuration is exactly the same as that for the symmetry experiments, as shown in Figures 1 and 2, except that a simplified fault has been added. As shown in Figure 6, the fault consists of two 6-inch-diameter (15.24 cm) parallel Mylar discs, each 5 mils (0.0127 cm) thick and 3/16 inch (0.476 cm) apart, and with the disc closer to the charge being 0.52 inch (1.34 cm) from the common center of the charge and cylinder. The normal to the disc is oriented at 45° to the vertical axis of the cylinder and lies in the vertical plane that contains the charge and bisects the particle velocity gages. In this position the fault bisects the radial line extending from the edge of the charge to the center of the active element of the particle velocity gage.

2.2 Particle Velocity Gage

The EF gage is shown schematically in Figure 7. It consists of a wire loop following the cylindrical coordinate system of the midheight plane of the grout cylinder. Because the polar coordinates coincide in this plane with the spherical coordinates, only that small arc marked 'active element' moves perpendicular to its own axis during the outward

passage of the wave, that is, before the wave reaches the outside of the grout cylinder. The solenoid surrounding the grout creates a constant magnetic field B with flux lines in an axial direction at the midheight plane. The active element of length $\ell = r(t)\,\theta$ moves radially at the particle velocity $v = dr/dt$ of the wave and cuts the axial flux lines ϕ encircled by the gage loop of area $A(t)$. This process induces in the gage loop a voltage ε proportional to the particle velocity. Thus

$$\varepsilon = \frac{d}{dt} = -\frac{d}{dt} BA(t) = -\frac{dA}{dt}$$

$$= B\theta r \frac{dr}{dt} = B\ell v$$

In the experiments, $B = 0.156$ w/m^2 and $\ell = 0.01$ m, so if the particle velocity is expected to be $v = 10$ m/s, the voltage signal is $\varepsilon = 0.015$ V. To provide a larger signal, the particle velocity was constructed of 18 loops; thus if the particle velocity is again 10 m/s, the corresponding voltage signal is 0.27 V.

2.3 Model Fabrication

Figures 8 and 9 show two views of an assembly before grout pouring for a symmetry experiment. The particle velocity gages and the Hall probes are supported in the midheight plane from the cylindrical Lucite mold. The charge is supported at the center on a stainless steel tube that is firmly attached to a wooden disc that forms the base of the mold. The steel tube protrudes through the wooden disc to serve as a suspension support for the grout cylinder (Figure 1) and as a convenient exit for the detonation leads; the gage and probe leads run axially close to the inside surface of the mold. Templates are used to accurately wind the 18 loops of the particle velocity gages and to position the gages and probes at the same distance from the charge. Figures 10 and 11 show two views of an assembly before grout pouring for an asymmetry experiment. The asymmetry model is the same as the symmetry model; only the fault has been added.

The grout was poured along with standard cylindrical samples for compression and splitting tests to verify quality assurance. After the grout had set adequately, the mold was removed and the model was subjected to a thermally accelerated curing process so that full grout strength was achieved in 14 days.

2.4 Auxiliary Tests

Three grout cylinders containing only the 3/8-gram charge were made for tests to determine the overburden pressure required to prevent overall cracking. With no overburden, the charge broke the cylinder into five major pieces. With an overburden of 500 psi (3.45 MPa), a single crack was produced but the cylinder remained in one piece. With an overburden of 1000 psi (6.90 MPa), no crack was produced. Although the particle velocity measurements were made during the outward propagation of the spherical wave and the cracking probably occurs after reflection from the grout surface, it was decided to pressurize the cylinders to 1000 psi (6.90 MPa) for the wave experiments for unambiguous interpretation of the velocity gage records.

In the first symmetry test, we noticed a damped oscillatory electrical noise in the particle velocity record that started immediately upon detonation of the explosive. After the test the steel tube was drilled out to provide access to the cavity formed by the explosive. A bridge wire (Figure 3) was inserted in the cavity and exploded by capacitor discharge. Electrical noise similar to that detected in the symmetry test was picked up immediately by the particle velocity gage. In this way, we were able to determine the noise to be subtracted from the signals in the four main tests. The noise was negligible by the time the peak particle velocity was attained.

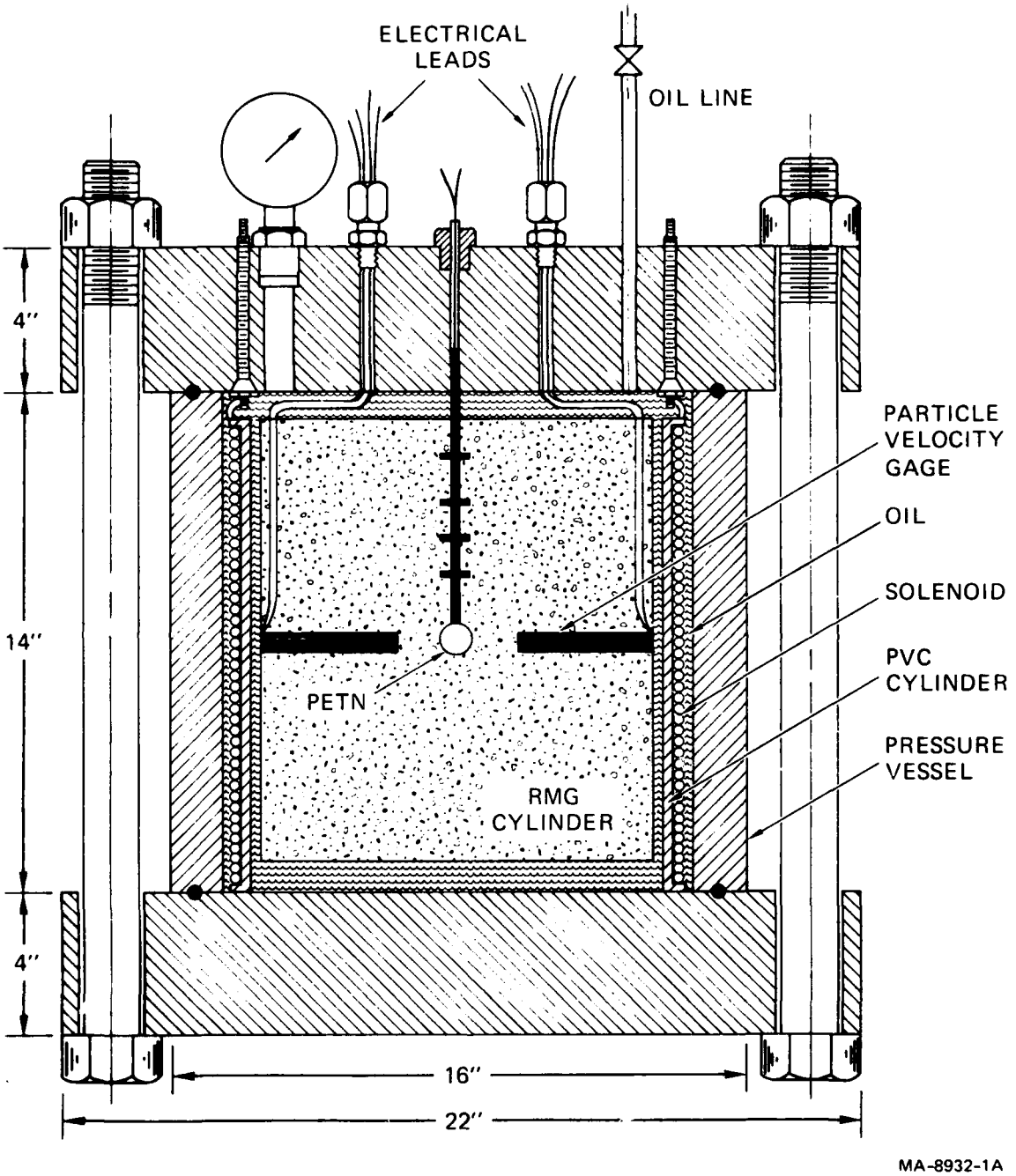

FIGURE 1 CONFIGURATION FOR SYMMETRY EXPERIMENTS
(Vertical Cross Section)

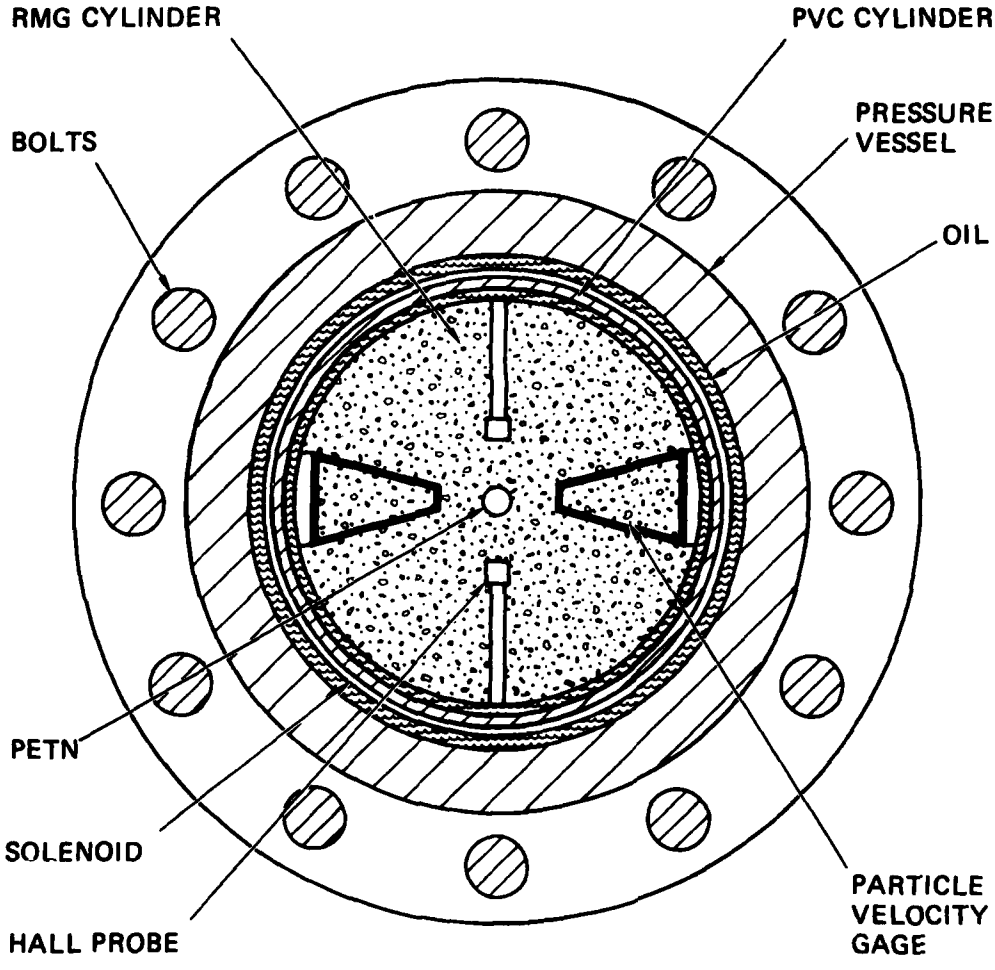

FIGURE 2 CONFIGURATION FOR SYMMETRY EXPERIMENTS
(Horizontal Cross Section)

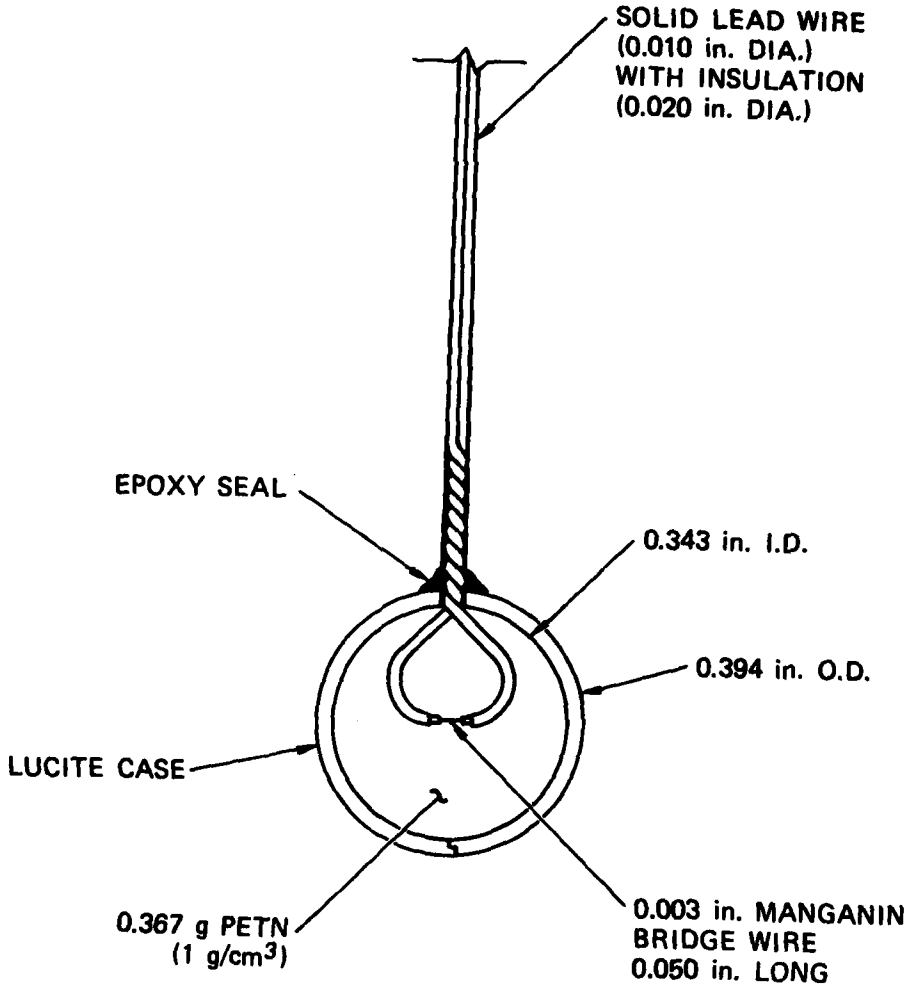

FIGURE 3 EXPLOSIVE CHARGE

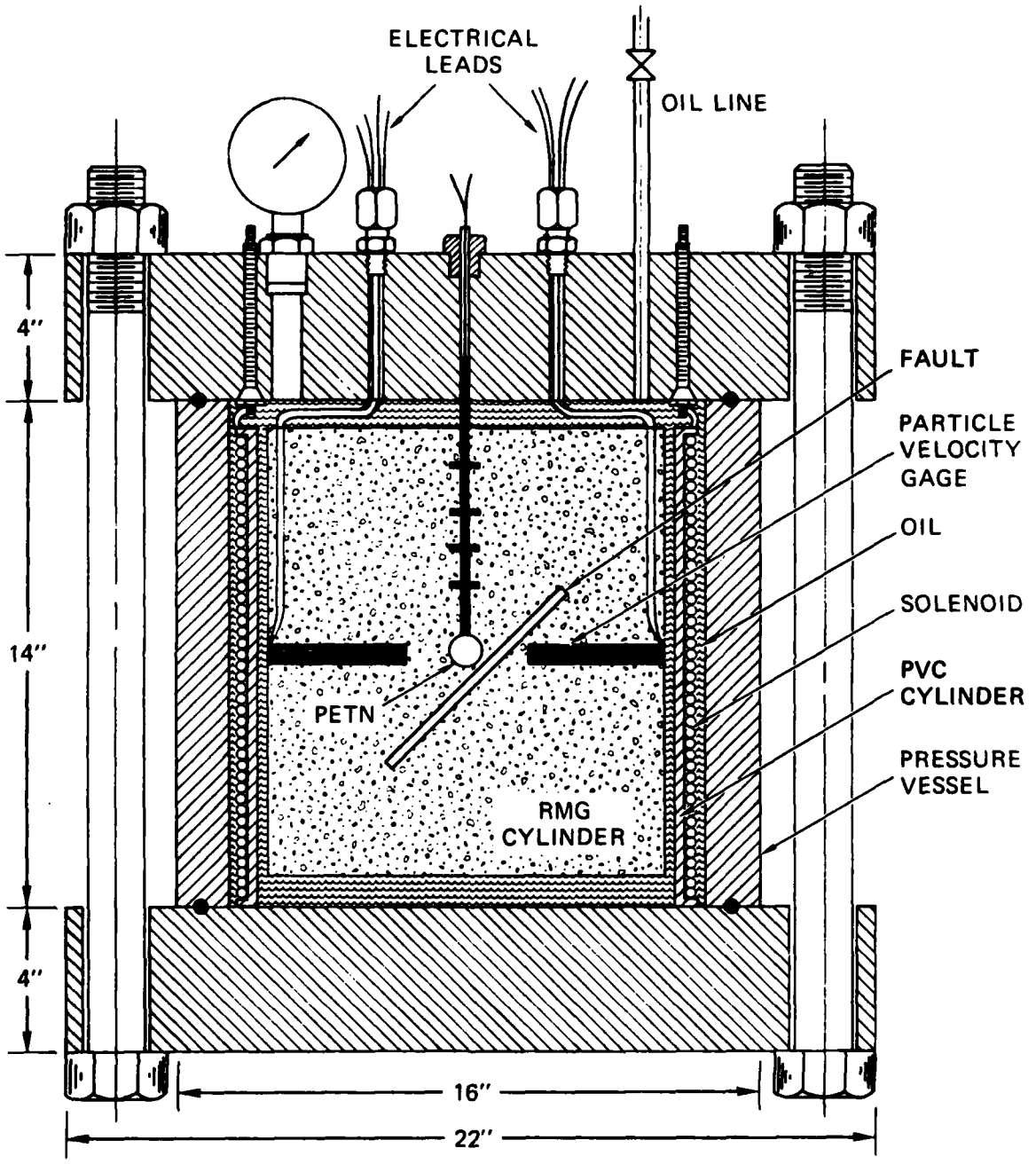

FIGURE 4 CONFIGURATION FOR ASYMMETRY EXPERIMENTS
(Vertical Cross Section)

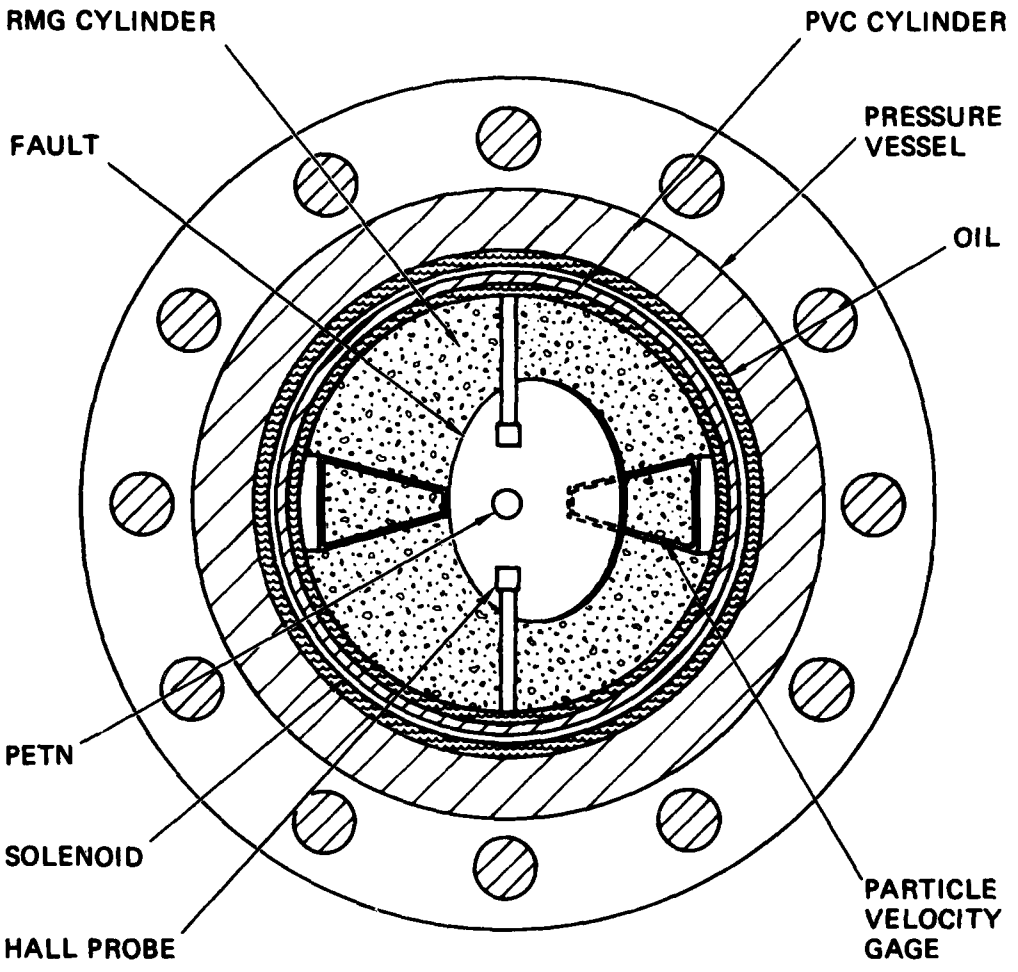

FIGURE 5 CONFIGURATION FOR ASYMMETRY EXPERIMENTS
(Horizontal Cross Section)

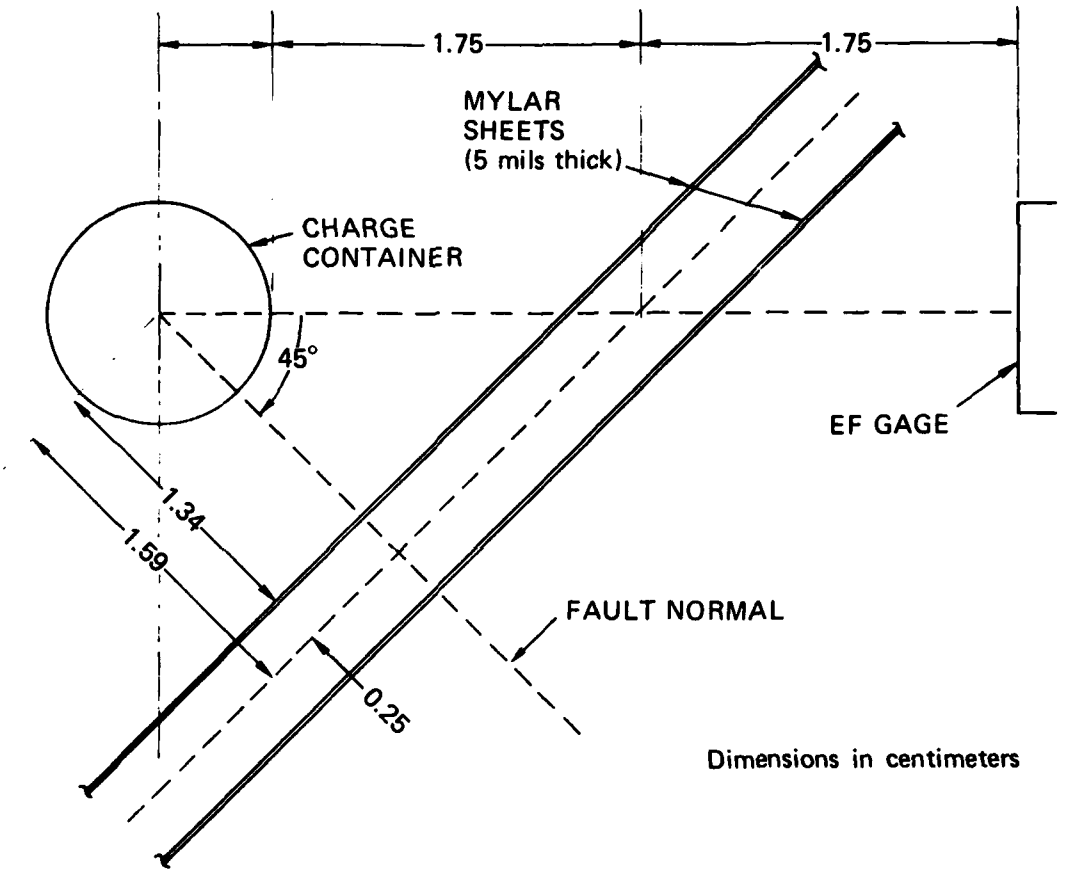

FIGURE 6 FAULT LOCATION
(Vertical Cross Section)

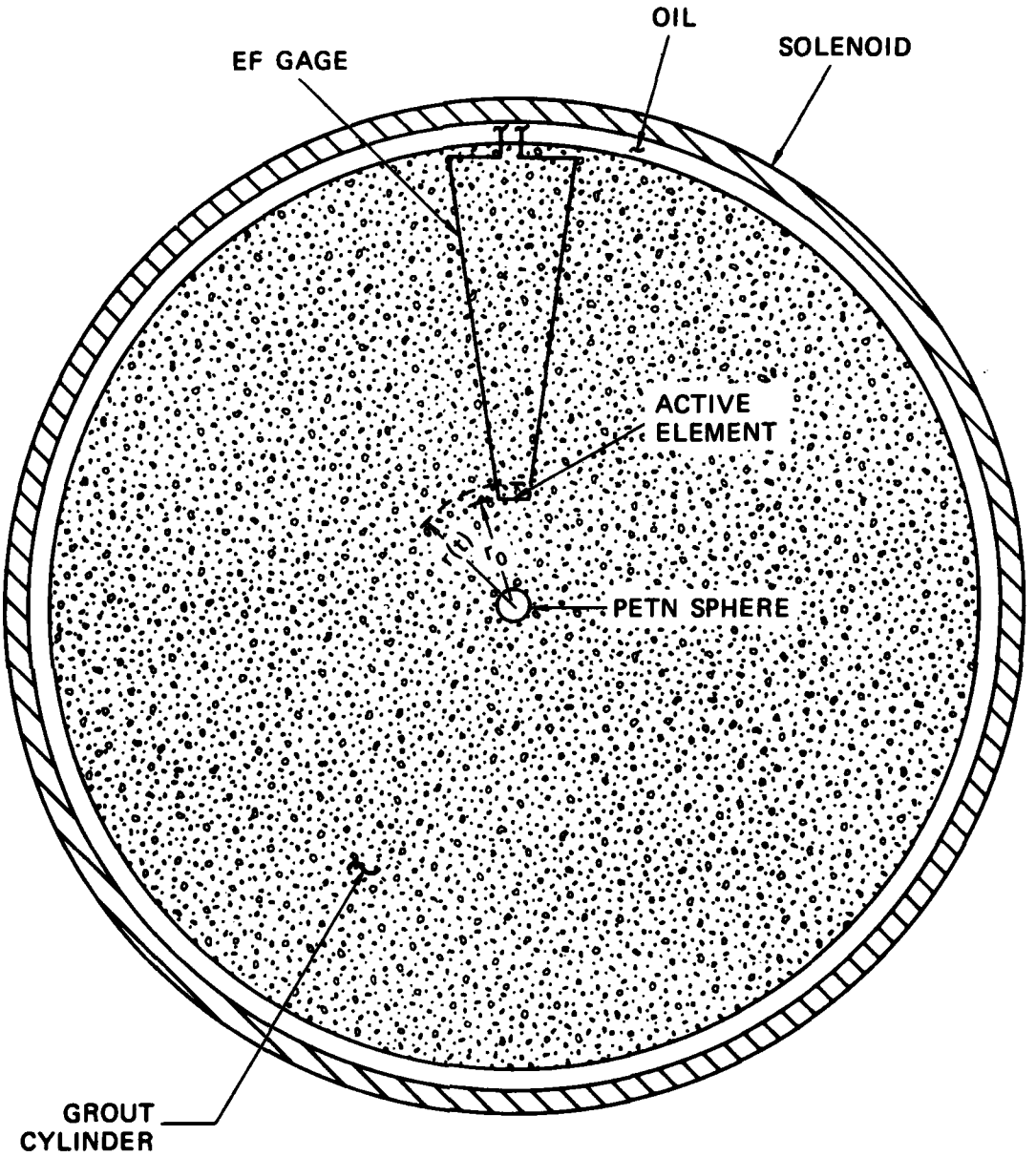

r_0 is initial position of active element

r(t) is current position of active element

MA-8392-2

FIGURE 7 EXTERNAL FIELD ELECTROMAGNETIC PARTICLE VELOCITY GAGE IN SYMMETRY EXPERIMENT

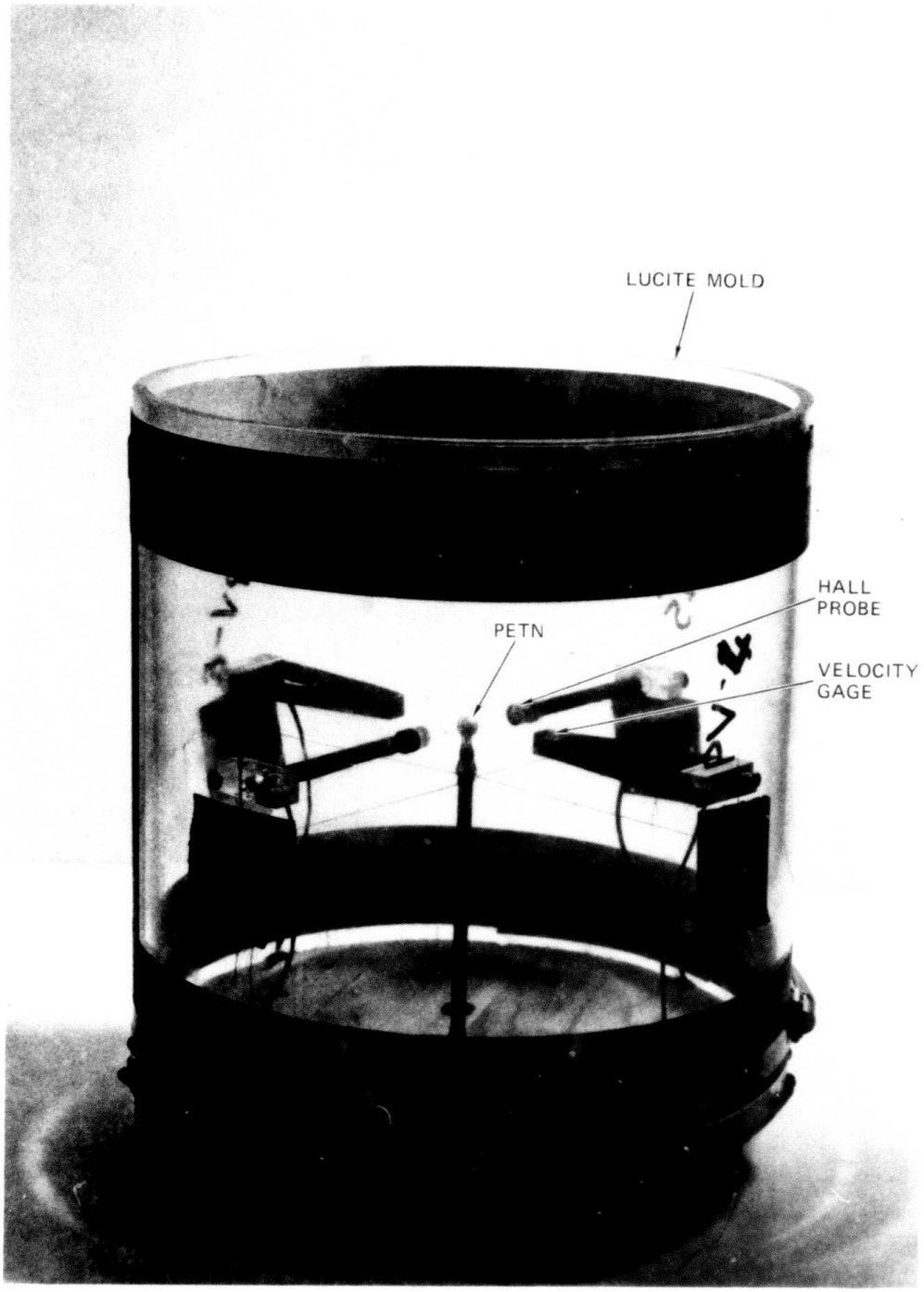

MP-8392-3

FIGURE 8 SIDE VIEW OF INSTALLATIONS BEFORE GROUT POURING FOR SYMMETRY EXPERIMENTS

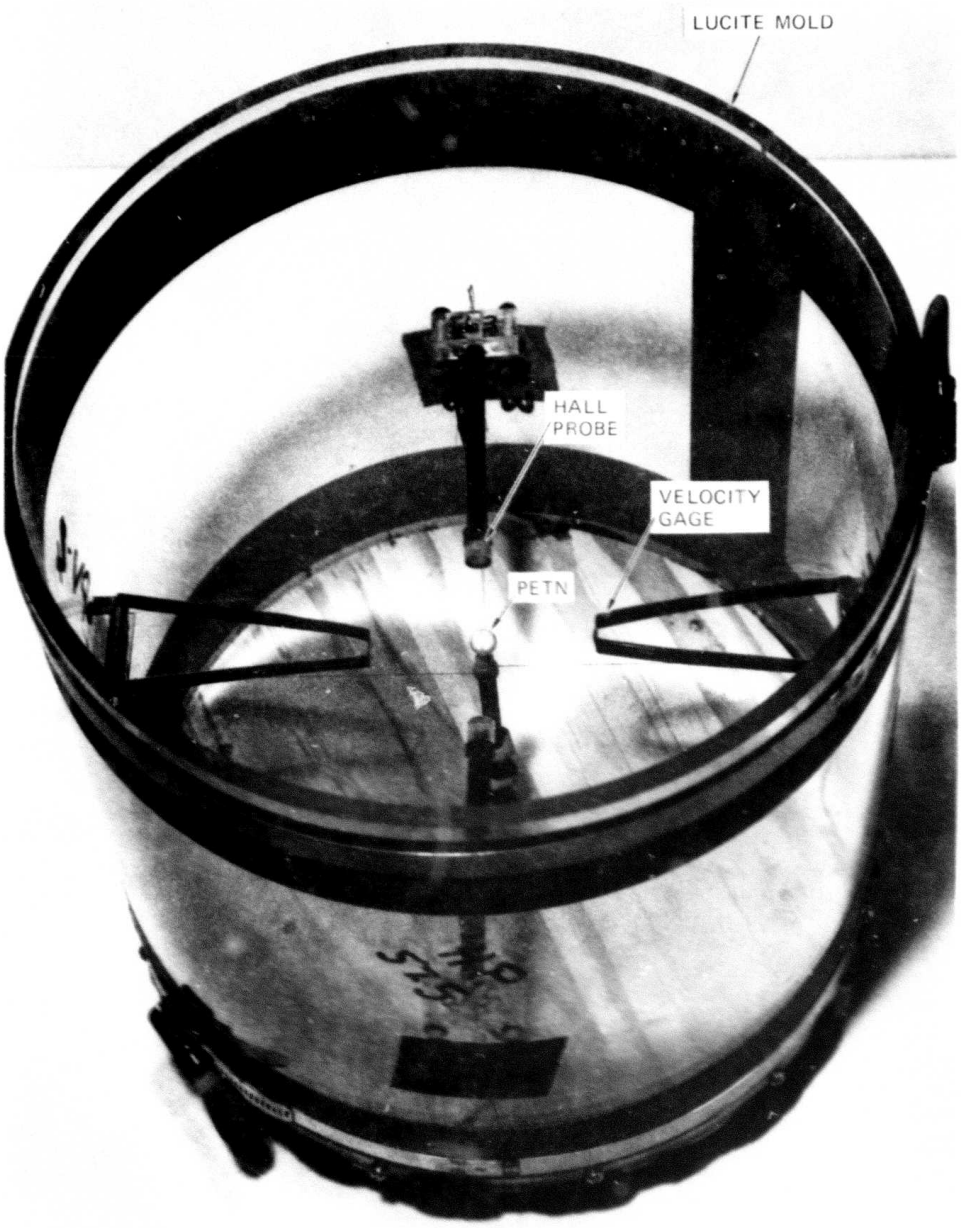

MP-8392-4

FIGURE 9 TOP VIEW OF INSTALLATIONS BEFORE GROUT POURING FOR SYMMETRY EXPERIMENTS

MP-8392-7

FIGURE 10 SIDE VIEW OF INSTALLATIONS BEFORE GROUT POURING FOR ASYMMETRY EXPERIMENTS

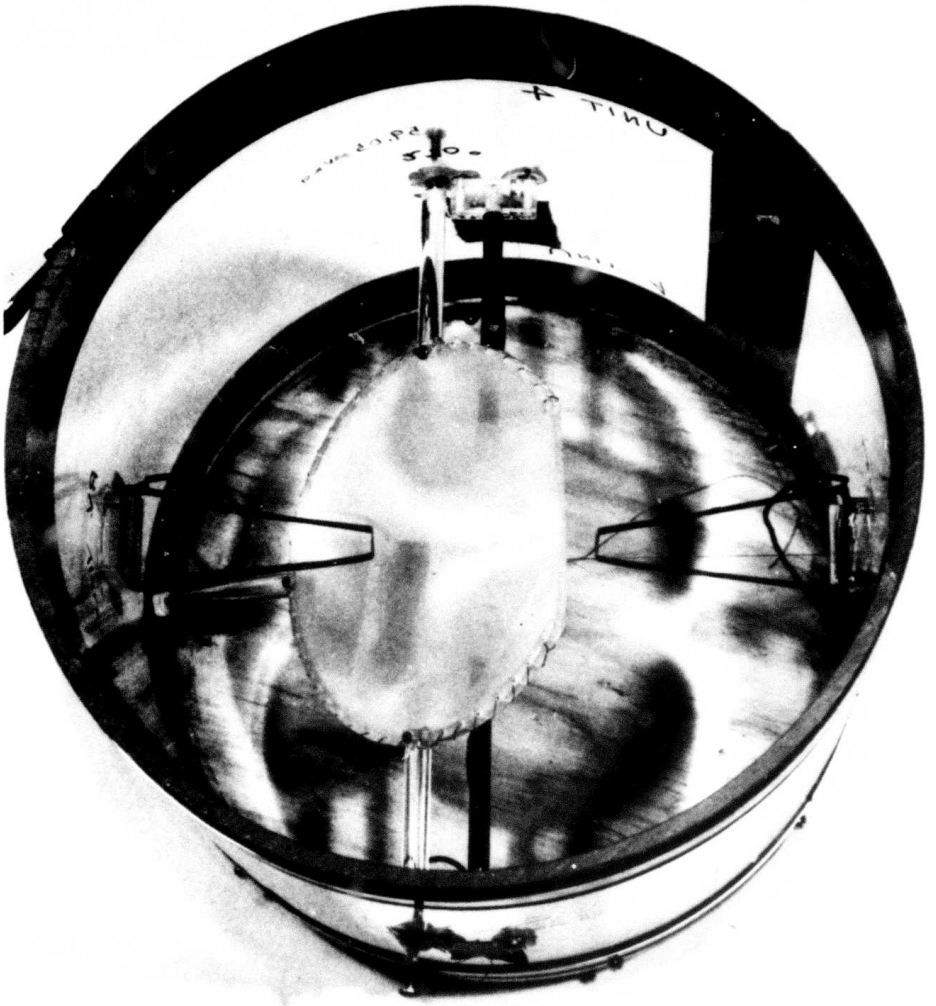

MP-8392-8

FIGURE 11 TOP VIEW OF INSTALLATIONS BEFORE GROUT POURING FOR ASYMMETRY EXPERIMENTS

3. EXPERIMENTAL RESULTS

Table 1 lists the main data for the five laboratory experiments performed: two symmetry experiments (without faults) and three asymmetry experiments (with faults), the configurations for which are shown in Figures 1, 2, 4, and 5. The average values of the solenoid current and resulting magnetic field are 414 A and 0.1506 W/m^2, respectively.

Figure 12(a) shows an oscillograph of the particle velocity record obtained from gage PV1 in symmetry Test 2. The spherical wave from the charge reaches the active element, located at a radius of 4 cm, 14 μsec after detonation. Figure 12(b) shows an oscillograph of the electrical noise obtained from the auxiliary test described in Section 2.4. By identifying the initial noise pulse in Figures 12(a) and 12(b), we can subtract the noise from Figure 12(a) to provide a record that is predominantly the velocity gage signal. Figure 13 shows the oscillographs from asymmetric Test 4; the oscillographs from Test 5 are similar. The noise level in these tests is low enough that it is sufficient simply to neglect the initial noise. After performing this subtracting process with the six corresponding particle velocity records of Tests 1, 2, 4, and 5, neglecting the initial residual noise, we obtain the particle velocity histories of Figure 14; the maximum values are listed in Table 1.

Figure 14 shows that the particle velocities for the spherically symmetric wave are reasonably reproducible. The average maximum value is 10.95 m/s, and the maximum and minimum values of the peaks are, respectively, 14.8% and 11.7% above and below the average value. The rise time and duration are all about 5 and 25 μsec.

The curves labeled 4 and 5 in Figure 14 were obtained from gage PV2, which monitored that part of the wave that did not cross the fault in Tests 4 and 5, respectively. These records are replotted in Figures 15 and 16 along with the corresponding records from gage PV1, which monitored

part of the wave that did cross a fault. In Test 4 the fault caused the peak velocity to be decreased from 11.21 m/s to 7.67 m/s, a decrease of 32%. The corresponding decrease in Test 5 was from 12.57 m/s to 11.41 m/sec, a decrease of 9%. The overall shapes of the velocity records are similar, except near the end of the incident pulse, that is, beyond 32 sec after detonation. Although particle velocities were not obtained in Test 3, the main characteristics appeared in the records. In fact, we think that the ratio of the peak particle velocities is correct (same scale distortion).

The maximum radial displacements are listed in Table 1. They were obtained from the areas under the velocity history curves in Figures 14, 15, and 16. The six symmetry displacement values have an average of 0.159 mm, and the maximum and minimum values are, respectively, 20.8% and 16.4% above and below the average value. The asymmetry displacement value obtained by integration of the particle velocity record from gage PV1 in Test 4 is 0.109 mm, whereas the symmetry value from gage PV2 in Test 4 is 0.145 mm. Thus the fault caused a 25% decrease in the radial displacement. The corresponding decrease in Test 5 was from 0.192 mm to 0.165 mm, a decrease of 14%.

We attribute the difference between the fault effects in Tests 4 and 5 to different fault slip characteristics introduced by using slightly different techniques for fault installation. In Test 4 the Mylar sheets were installed with an air space that was filled during grout pouring for the entire cylinder. In Test 5 the space between the Mylar sheets was filled with grout and cured before the sheets were installed in the cylinder. In the future, we recommend that a simpler single fault be used.

Table 1

EXPERIMENTAL DATA

	Symmetry		Asymmetry		
	Expt 1	Expt 2	Expt 3	Expt 4	Expt 5
Solenoid current (A)	416	410	424	414	407
Magnetic field (W/m^2)					
HP1	0.1334	0.1468	0.1739	0.1718	a
HP2	0.1393	0.1415	b	0.1473	a
Maximum particle velocity (m/s)					
PV1	12.10	9.67	c	7.67	11.41
PV2	10.33	9.81	c	11.21	12.57
Maximum displacement (mm)					
PV1	0.180	0.133	c	0.109	0.165
PV2	0.158	0.153	c	0.145	0.192
Velocity ratio PV1/PV2	1.17	0.99	0.81	0.68	0.91
Displacement ratio PV1/PV2	1.14	0.84	c	0.75	0.86

[a] Hall probes not used: theoretical B = 0.151 W/m^2 used.

[b] No record.

[c] Excessive noise.

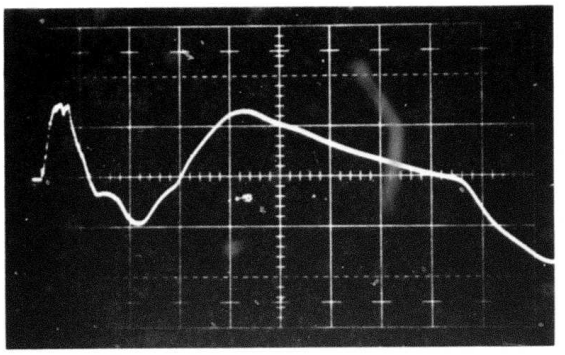

(a) PARTICLE VELOCITY RECORD FOR TEST 2 (Gage PV1)

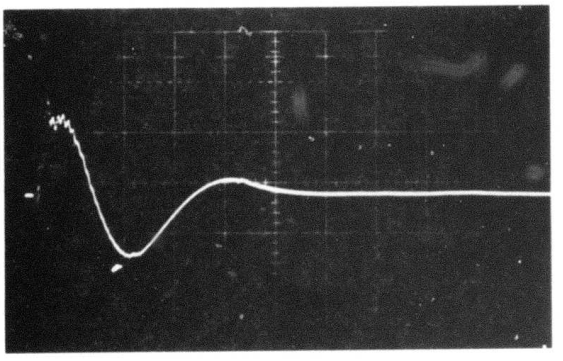

(b) NOISE CALIBRATION TEST

MP-8392-10

FIGURE 12 PARTICLE VELOCITY (TEST 2) AND NOISE RECORDS

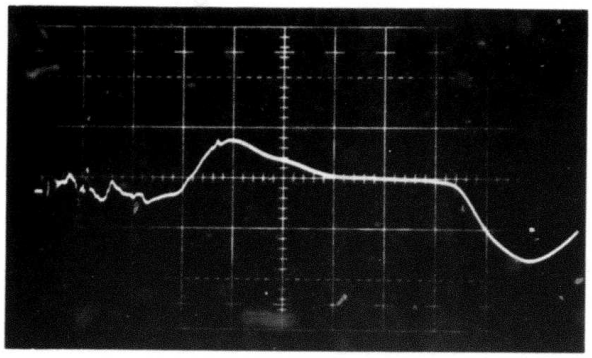

(a) PARTICLE VELOCITY RECORD FOR TEST 4 (Gage PV1)

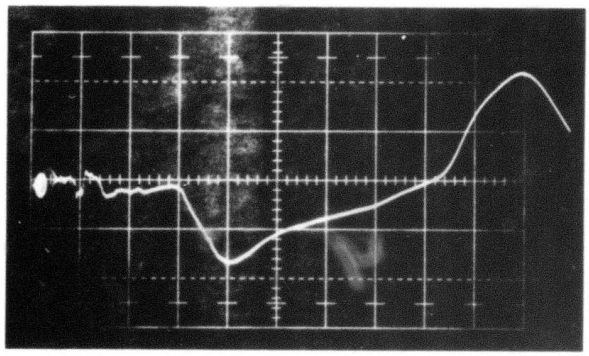

(b) PARTICLE VELOCITY RECORD FOR TEST 4 (Gage PV2)

MP-8392-11

FIGURE 13 PARTICLE VELOCITY RECORDS FROM TEST 4

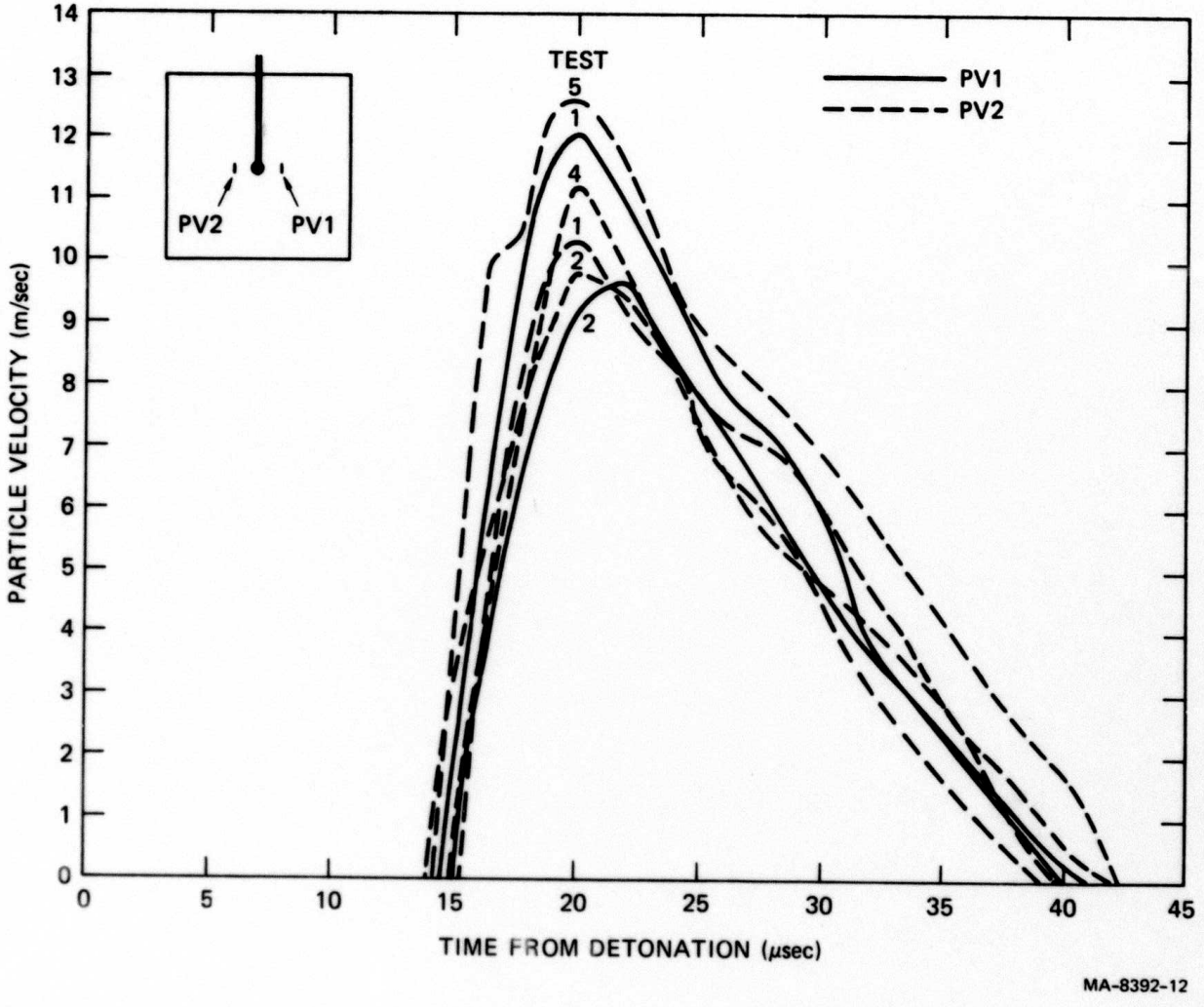

FIGURE 14 SYMMETRY PARTICLE VELOCITY PLOTS

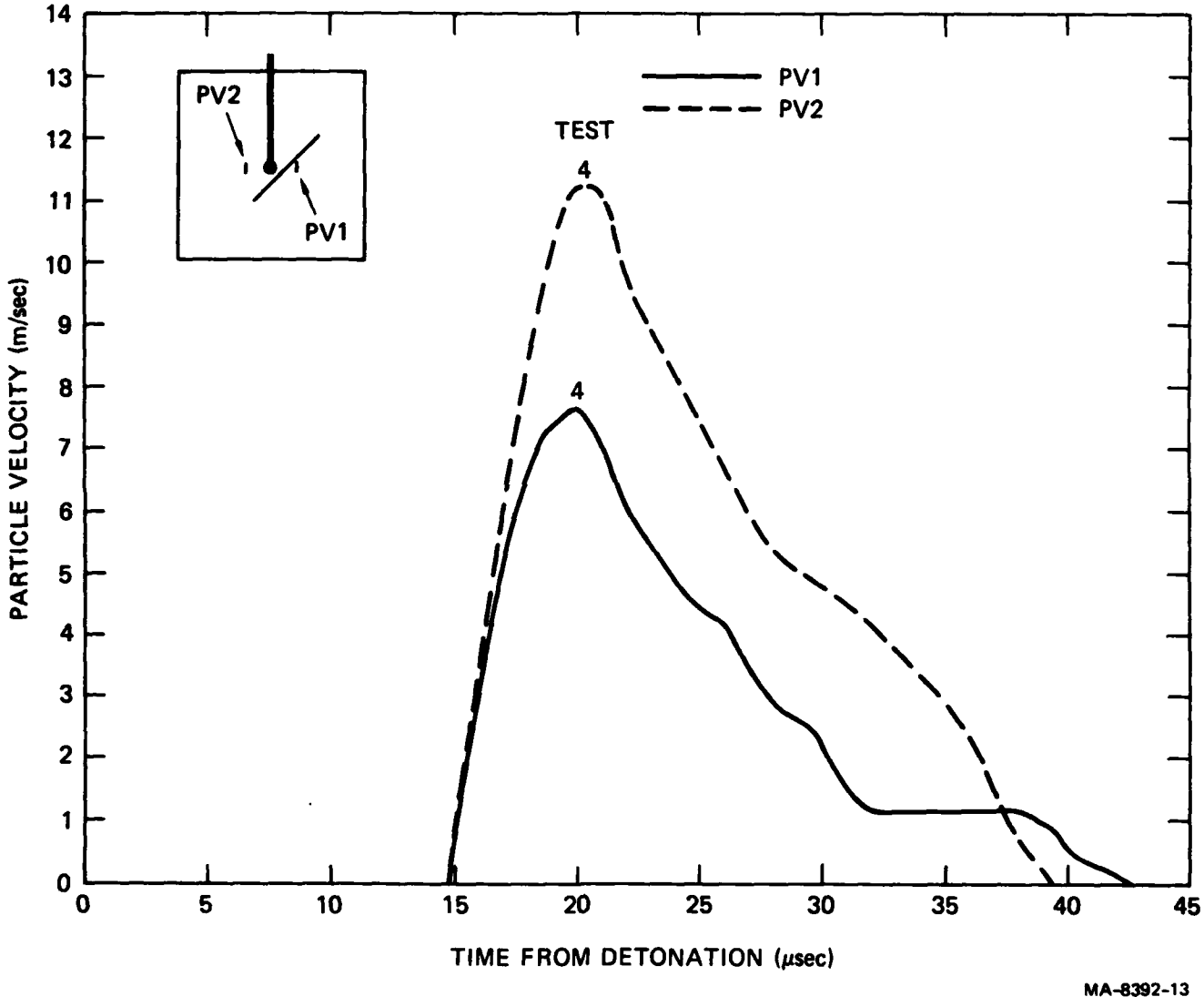

FIGURE 15 PARTICLE VELOCITY PLOTS OF ASYMMETRY TEST 4

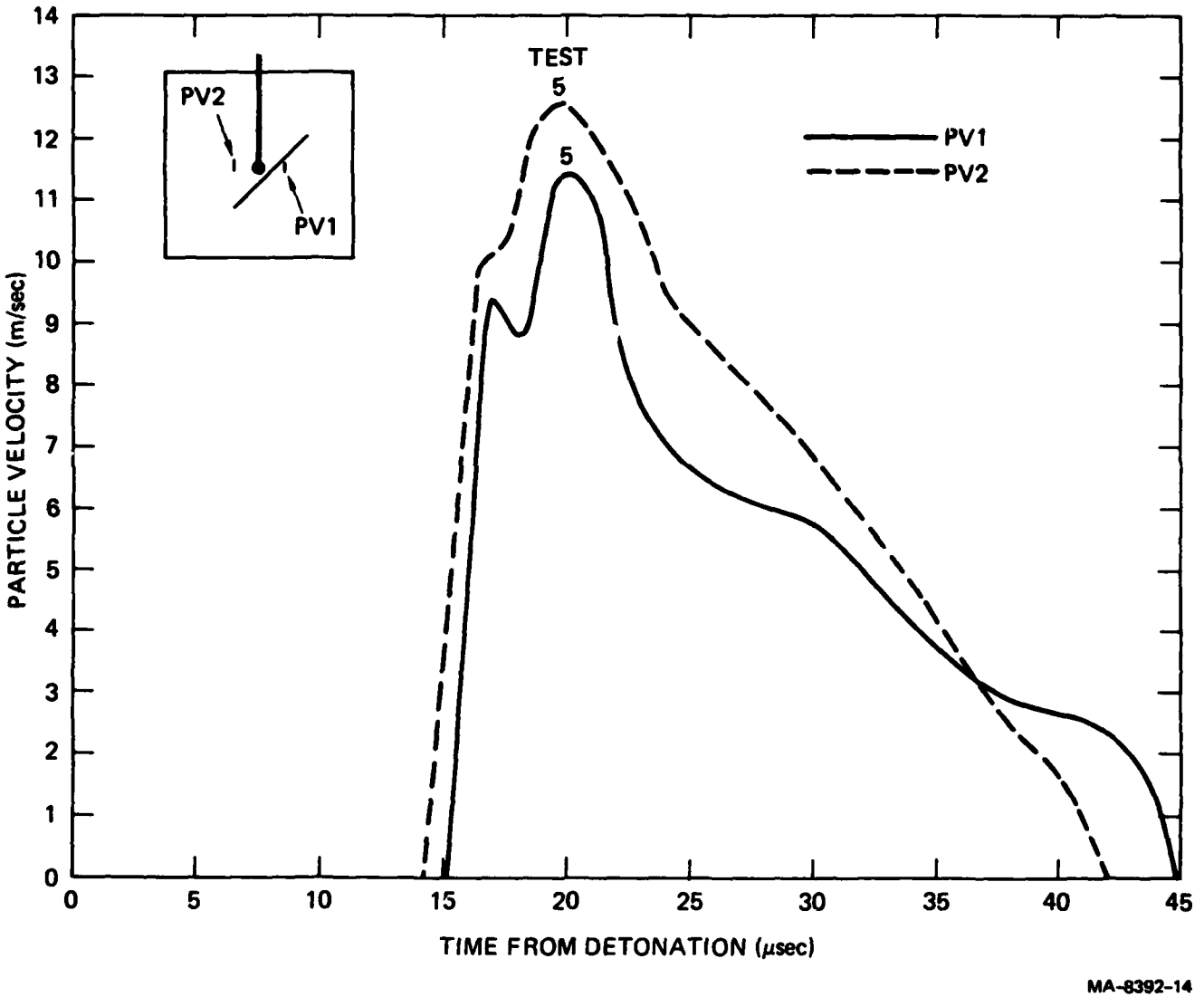

FIGURE 16 PARTICLE VELOCITY PLOTS OF ASYMMETRY TEST 5

4. RECOMMENDATIONS

We recommend that the technique be improved by increasing the signal-to-noise ratio. Possible measures that could be taken to achieve this improvement are to

- Increase the magnetic field of the solenoid by adding more batteries or by incorporating a pulsed field and detonating the charge when the field is a maximum.
- Determine and use the orientation of the wire loop at the bridgewire that minimizes noise reception in the particle velocity loops.
- Possibly detonate the charge with an explosive line that has an extremely small linear explosive density (for example, 1 grain/foot mild detonating fuze).
- Incorporate shielding of the source.

We recommend that more experiments on faults be performed for confirmation and to determine the degree of reproducibility.

We expect that the results on the effects of faults on spherical waves would be confirmed, in which case the technique would be available for such investigations as

- Generating additional data on the effects of faults by adding several particle velocity gages in each experiment.
- Studying wave-fault interactions in different materials (for example, granite simulant).
- Using wave-fault triggering of block motion to release tectonic strain energy.

Appendix

THE MUTUAL INDUCTANCE GAGE

Here we provide a description of the mutual inductance particle velocity gage (MI gage) and show why this gage was not suitable for our spherical wave experiments.

An idealized two-loop version of the mutual inductange gage[2-5] is shown in Figure A.1. The gage is assumed to be Lagrangian by virtue of its elements being very thin and weak so that they will quickly equilibrate with the flow. A constant current I is flowed through the primary (or current) loop, and as the gage deforms, an electromotive force $\varepsilon(t)$ is induced across the secondary (or sensor) loop. Using the basic equations of electromagnetic theory, we may express the gage output $\varepsilon(t)$ as

$$\varepsilon(t) = -\frac{d\phi}{dt} = -\frac{d}{dt}(MI) = -I\frac{dM}{dt} \tag{1}$$

where ϕ is the magnetic flux linking the sensor loop and M is the mutual inductance between the loops.

For planar (uniaxial) flow, M is a function of a single spatial coordinate x(t) defined in Figure A.1. Therefore, equation (1) may be simplfied to obtain a direct relation between the gage output $\varepsilon(t)$ and the desired Lagrange particle velocity at the front of the gage u(t):

$$\varepsilon(t) = -I\frac{dM}{dt} = -I\frac{dM}{dx}\frac{dx}{dt} = \left[-I\frac{dM}{dx}\right]u(t) \tag{2}$$

where the term inside the brackets is essentially constant.[4]

In the present case, however, the flow is divergent, so M is not a function of x(t) only. Consequently, there is no simple relationship,

such as equation (2), relating the gage output to the Lagrange radial particle velocity. To determine the gage response in spherical flow, we solved equation (1) numerically by evaluating and differentiating M(t) from its general defining equation

$$M(t) = \frac{\mu_o}{4\pi} \oint\oint \frac{\vec{dl}_p(t) \cdot \vec{dl}_s(t)}{r(t)} \qquad (3)$$

where μ_o is the permeability, $\vec{dl}_p(t)$ and $\vec{dl}_s(t)$ are vector elements of the current and sensor loops, r(t) is the separation between them, and the integrations are closed line integrals around each loop. A mutual inductance gage computer code was modified and used for this purpose. The configuration of the gage as a function of time throughout the experiment is required as input for the mutual inductance gage code. We obtained this input by simulating the experiment with the SRI spherical PUFF code, a one-dimensional artifical viscosity Lagrangian wave propagation code.

A series of calculations with the mutual inductance code showed that, with gages of the dimensions required for the present experiments (separation a is small compared with the width b and the length x, Figure A.1.), the gage signal $\varepsilon(t)$ is dominated by changes in the coil separation, a, rather than by the radial particle velocity u(t). This behavior results because the magnetic field produced by the current loop elements and experienced by the sensor loop elements is a strong function of distance between the elements [see equation (3)]. Because this behavior is an inherent property of mutual inductance gages in spherical flow, the mutual inductance gage was judged unsuitable for the present program, and an alternative Lagrangian particle velocity gage was developed.

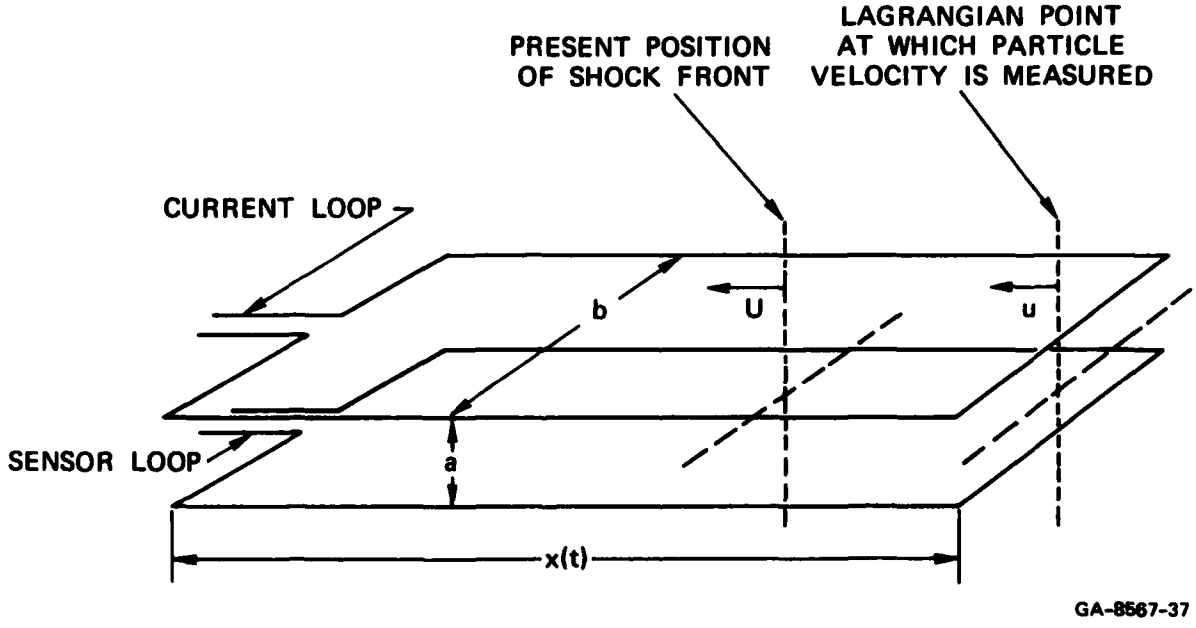

FIGURE A.1 IDEALIZED GEOMETRY FOR MUTUAL INDUCTANCE GAGE
U is the shock velocity and u is the particle velocity.

REFERENCES

1. J. C. Cizek and A. L. Florence, "Laboratory Studies of Containment in Underground Nuclear Tests," Draft Final Report, DNA 0000F (January 1979).

2. D. D. Keough and A. L. Florence, "Experimental Study of the Effects of Faults on Spherical Wave Propagation, Phase I," SRI International Research Proposal No. PYU 78-226 (September 1978).

3. W. L. Danek, D. J. Schooley, and F. A. Jerozal, "Particle Velocimeter for Use Close in to Underground Explosions," Final Report DASA-1431-3 (October 1967).

4. D. E. Grady, C. W. Smith, and L. Seaman, "In Situ Constitutive Relations of Rocks," DNA 3172Z (January 1973).

5. J. T. Rosenberg, C. W. Smith, and D. R. Curran, "In Situ Constitutive Relations of Soils and Rocks," Final Report DNA 4097F (1976)